CO + H SUB 2 REACTION OVER NITROGEN-MODIFIED IRON CATALYSTS. QUARTERLY TECHNICAL PROGRESS REPORT, OCTOBER 1, 1983-DECEMBER 30, 1983
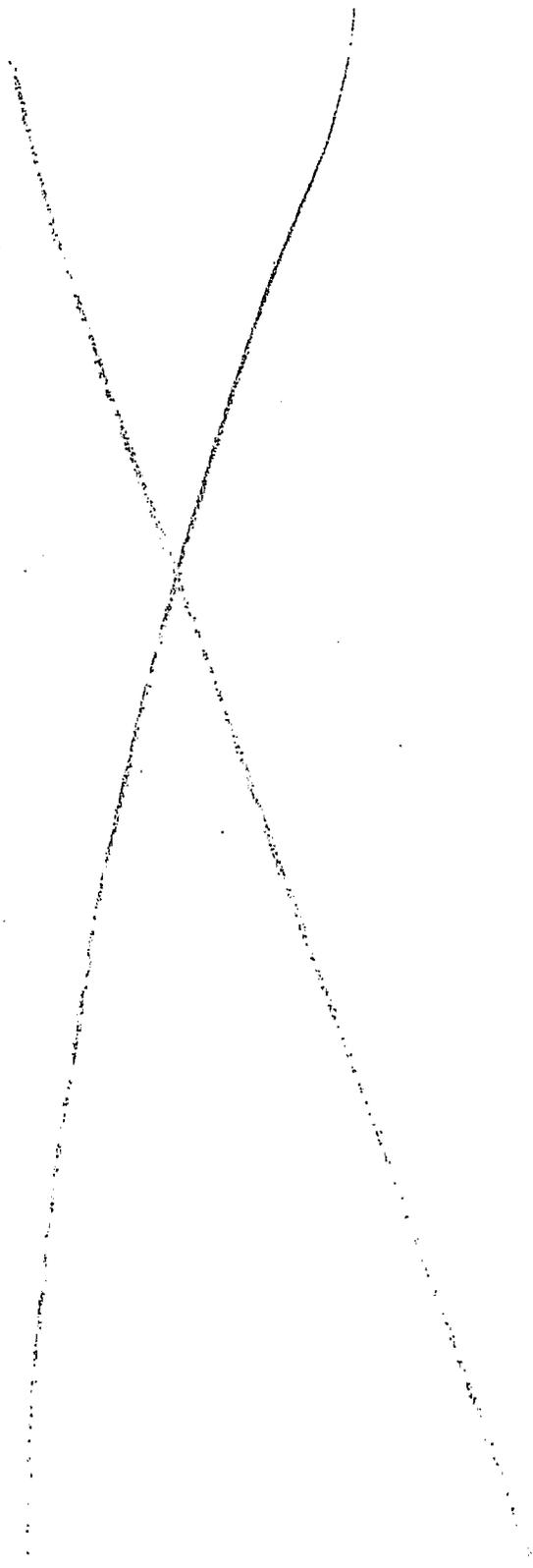
PURDUE UNIV.
LAFAYETTE, IN

FEB 1984

CO + H$_2$ Reaction Over

Nitrogen-Modified Iron Catalysts

Quarterly Technical Progress Report
for the Period Oct. 1, 1983 - Dec. 30, 1983

W. Nicholas Delgass
Purdue University
West Lafayette, Indiana 47907

PREPARED FOR THE

U. S. DEPARTMENT OF ENERGY

TABLE OF CONTENTS

LIST OF FIGURES

ABSTRACT

The synthesis of ϵ-Fe$_{2.7}$N is confirmed by Mössbauer spectroscopy. Carburization of ϵ-iron nitride for 2.5 hours in 3H$_2$/CO at 523 K starts the formation of a bulk structure similar to that seen during γ'-iron nitride carburization. Reaction of γ'-Fe$_4$N in 3CO/H$_2$ synthesis gas at 523 K shows a better bulk stability than reaction in 3H$_2$/CO. Kinetic analysis of the product distribution at the higher CO ratio confirms greater activity and selectivity maintainance.

The kinetics of denitriding in both He and H$_2$ was studied with a mass spectrometer. Extremely rapid nitrogen loss was observed from both γ'-Fe$_4$N and ϵ-Fe$_{2.7}$N catalysts in H$_2$ at 523 K. In both cases a initial exposure to H$_2$ produced a significant amount of NH$_3$ which we ascribe to an active surface species. Hydrogenation of the bulk continued with a slow rise to a maximum about 90 seconds after the introduction of H$_2$. The denitriding activity of the ϵ-Fe$_{2.7}$N catalyst was significantly higher than that of the γ'-Fe$_4$N catalyst. In contrast, the denitriding rate of ϵ-Fe$_{2.7}$N in He was significantly slower than that in H$_2$ until high temperatures (773K) were reached. An overall activation energy of 41.5 kcal/mol was obtained for this process.

Comparison of the denitriding rate of virgin ϵ-Fe$_{2.7}$N in H$_2$ with that of the same nitride after five minutes of carburization during the hydrocarbon synthesis reaction indicates large differences in the overall rate. The carburized nitride was some 300

times less active to bulk hydrogenation than the virgin catalyst, which is indicative of significant changes in the first few layers of the nitride during the initial minutes of the synthesis reaction.

1. OBJECTIVES AND SCOPE

1.1 BACKGROUND

The feasibility of utilizing synthesis gas $(CO + H_2)$ via the Fischer-Tropsch reaction pathway for the production of fuels and chemicals is well established. The SASOL ventures, for example, take advantage of abundant coal resources to produce both desirable synthetic automotive fuels and basic chemical feedstocks. The applicability of these chemical transformations is nonetheless limited. The present procedure requires extensive processing if the production of non-essential byproducts is to be avoided. The discovery and subsequent usage of improved catalysts would therefore be advantageous.

Experimental results published in the current literature show that nitrogen affects the performance of iron catalysts-catalysts which find widespread use in the Fischer-Tropsch synthesis route. Prenitriding of the fused promoted iron and precipitated iron catalyst is said to shift the product distribution to one exhibiting lower molecular weight fractions and enhanced alcohol yields (1,2). Iron nitrides with high initial activity and significant stability over weeks of experimentation are also reported (1,2). On the other hand, simultaneous introduction of ammonia (NH_3) with synthesis gas produces nitrogeneous compounds. Furthermore, and probably of greater importance, this addition of ammonia effects a reduction in the overall chain length of compounds in the product spectrum (3,4). It is of considerable

interest, therefore, to study these and other characteristics of
nitrided iron catalysts in order to gain a basic understanding of
their behavior. Discovery of the new pathways in Fischer-Tropsch
synthesis afforded by nitrogen will add to the fundamental
knowledge from which future synthesis-catalysts can be derived.

1.2 OBJECTIVES

The scope of the program may be broken down into two main
areas of concern. Firstly, consideration must be given to the
role of the surface nitrogen in

i. altering the product distribution and

ii. stabilizing catalyst activity

of the synthesis reactions. In-situ Mössbauer studies, are aid-
ing in the identification of the various iron nitride phases and
allow examination of their stability during reaction. The
Mössbauer results are forming a the basis for detailed kinetic
tracer experiments involving transient and isotope labeling ana-
lyses. Ultrahigh vacuum work using SIMS and AES will supplement
the Mössbauer and kinetic characterizations. XRD studies will
supplement the Mössbauer effect in identifying the bulk iron
nitride phases.

The second area of consideration will involve the kinetic
and catalytic effects observed during the addition of ammonia to
the synthesis gas stream. Transient work will be ideal for
observing initial activity changes occurring as a result of NH_3

pulses. Along with ultrahigh vacuum studies, the transient kinetics of NH_3 addition will help clarify which steady state experiments would be most productive. The various analytical methods will define interactions between surface and bulk nitrogen, and their role in effecting new reaction pathways.

The primary experiments which define our route to understanding which parameters influence the selectivity and alter the activity of synthesis reactions may, therefore, be outlined as follows:

i. Mössbauer and simultaneous kinetics of prenitrided iron catalysts are being used to determine nitride phase stability and to correlate these phases to reaction selectivity.

ii. Similar analysis of the effects of addition of NH_3 to the reactant stream will be performed.

iii. Transient analysis and isotope tracer studies of synthesis reactions over prenitrided catalysts will determine surface nitride stability. The stoichiometry at the surface and influence of nitriding on CO dissociation will be sought.

iv. Ultrahigh vacuum analysis will examine surface stoichiometry and reaction intermediates. Interaction between the nitrided phases and adsorption bond strengths of CO and H_2 will be investigated.

v. The effects of NH_3 addition to the reactant stream will
be similarly followed by UHV and transient tracer stu-
dies to determine possible alterations in reaction
pathways invoked by the presence of NH_3.

Computer modeling will be undertaken to aid in quantitative
interpretation of transient data.

2. TECHNICAL PROGRESS

2.1 LITERATURE REVIEW

2.1.1 Iron Nitride Decomposition

Decomposition of iron nitrides subjected to various gas
atmospheres has received some attention in the literature. The
interaction (adsorption and desorption) of NH_3 from single cry-
stalline iron surfaces provides an approximation of the behavior
of nitrogen with polycrystalline iron surfaces. Grunze et al.
(5) studied the interaction of ammonia with Fe(111) and Fe(100)
surfaces with UPS, AES, LEED, TPD and work function measurements.

Their measurements of thermal desorption of ammonia from
Fe(111) showed three adsorption sites $(\beta_1, \beta_2$ and $\beta_3)$ at 160, 210
and 330 K respectively. The two lower temperature sites
$(\beta_1$ and $\beta_2)$ indicate coverage independent first order desorption
kinetics with activation energies of about 10 and 12.5 kcal/mol
respectively. The β_3 stage is attributed to the recombination of
NH_x ad and $(3-x)$ H_{ad}. The coverage dependency of the β_3 state

temperature indicates a second order rate process. The activation energy is estimated to be 20 kcal/mol, is agreement with the 25 kcal/mol estimate by Gay et al. (6) for this most tightly held site. The Fe(100) surface behaved similarly but uncertainties during data acquisition precluded definitive numerical assignments.

Drechsler (7) studied adsorption and decomposition of NH_3 from Fe(110) surfaces at temperatures from 130 K to 800 K with SIMS. Exposure of a clean Fe(110) surface to ammonia at temperatures between 130 K and 275 K produced non-dissociative NH_3 adsorption. Ammonia desorption (or complete dissociation) was essentially complete above 365 K. These SIMS studies showed adsorbed NH to be significantly more prevalent upon the Fe(110) surface than adsorbed NH_2. Grunze et al. (5) were unable to separate NH_{ad} from $NH_{2\ ad}$ with UPS 'fingerprints'.

Ertl and co-workers (8) followed the decomposition of ε and γ' surface nitrides (chemisorbed nitride) and nitride layered iron foils by means of AES, XPS and TPD measurements. The properties of $\gamma'-Fe_4N$ and $\varepsilon-Fe_{2-3}N$ surface nitrides should permit correlation to the stability of bulk iron nitrides. The authors state that thermodynamic considerations allow formation of both ε and γ' surface nitride (chemisorbed) layers from NH_3 provided the H_2 partial pressure is sufficiently small. AES and XPS spectra of iron surfaces, exposed to pressures of ammonia at various temperatures for different durations, show surface nitrogen and iron concentration equivalent to stoichiometric $\gamma'-Fe_4N$ and $\varepsilon-Fe_2N$.

An ε-Fe$_2$N sample was monitored by Auger spectroscopy. The surface layer nitrogen concentration exhibited plateaus; an initial ε-Fe$_2$N layer giving way to a γ'-Fe$_4$N layer and finally an α-Fe layer saturated with dissolved N atoms. Thermal desorption spectra of N$_2$ from a polycrystalline Fe$_4$N sample showed single broad desorption peaks corresponding to 54±3 kcal/mol (for first order desorption and a 10^{13}sec^{-1} pre-exponential). Annealing an iron sample, before thermal desorption, added a second higher temperature desorption peak to the spectra, a peak attributed to N diffusing from the sample bulk. Thermal desorption from ε-Fe$_2$N on the other hand produced a N$_2$ desorption peak at 700 K rather than that at approximately 850 K for the γ' nitride. An Arrhenius plot for the first order decomposition of several ε-nitrides yielded activation energies of 27±3 kcal/mol. Indications are, therefore, that Fe$_4$N is more stable than ε-Fe$_2$N.

Goodeve and Jack (9) and subsequently Jack (10) studied the kinetics of nitrogen evolution from iron-nitrogen interstitial alloys, particularly ε-iron nitrides. Each followed rates of denitriding of high N containing ε-iron nitride powders in vacuo, in nitrogen, in carbon monoxide and in hydrogen. The in vacuo experiments denote pressures below 20 torr. In both works (9,10) Jack concluded that the denitriding of ε-iron nitride proceeded at almost identical second order rates in vacuo, or in one atmosphere of either nitrogen or carbon monoxide. The rate controlling process would probably be the same in each experiment. Preliminary results also confirmed that the condition of the

alloy surface was an important rate determining feature.

Denitriding in a hydrogen atmosphere proceeded at rates faster, by a factor of 10^3-10^4, than denitriding under inert conditions. This increased reaction rate in H_2 precludes nitrogen diffusion from being the single slow step. Jack attributed the slow rate of recombination of pairs of nitrogen atoms at the solid surface to be the probable rate controlling step under inert conditions. Engelhard and Wagner (11) similarly concluded that the rate for the reaction

$$N(dissolved\ in\ \alpha-Fe) + 3/2H_2(g) -> NH_3(g)$$

was controlled by the reaction

$$N(dissolved\ in\ \alpha-Fe) + H_2(g) -> NH_2(a)$$

rather than bulk N diffusion through the bulk.

Jack (10) calculated the activation energy for the hydrogen assisted denitriding of e-iron nitride to be approximately 12 kcal/mol from initial rates in the temperature range 250-350°C. The second order rate of nitrogen evolution in a non-hydrogen atmosphere at 350-500°C was associated with an activation energy of 42.1±1.4 kal/mol.

2.1.2 Iron Nitride Kinetics

Highlights of iron nitride kinetic characteristics under

various synthesizing and carburizing atmospheres has been
reported previously (12). This section will summarize those
results and include recent work by Yeh et al. (13). The authors
reported on the promotion effects of potassium and nitrogen on
the activity and selectivity of silica supported iron.

Reactions were investigated at $250^{\circ}C$ and at pressures of
1.0, 7.8 and 14.0 atm. At 7.8 atm and $3H_2/CO$ both potassium pro-
moted and non-promoted iron catalysts (nitrided and non-nitrided)
showed good stability without carbon monoxide turnover frequency
deterioration between 3 and 12 hours. At approximate gas hourly
space velocities (GHSV) of 250 hr^{-1} both the iron nitride and K
promoted nitride showed decreasing ethylene and propylene selec-
tivities whereas the selectivities for unpromoted Fe were roughly
constant. The nitride olefin to paraffin ratios did, however,
remain higher than the corresponding ratio for iron. This ten-
dency in ethene/ethane ratio was maintaind at 14 atm between pro-
moted and unpromoted iron nitrides as against the corresponding
promoted and unpromoted iron. This trend reversed with the pro-
moted catalysts at one atmosphere, indicating the pressure sensi-
tivity of the C_2 selectivities. Yeh and coworkers (13) also stu-
died the production of methanol and ethanol during synthesis
reactions over their silica supported catalysts. Although
alcohol production from iron based synthesis catalysts is small
at one atmosphere, production becomes more prominent at higher
pressures. At 7.8 atm. with 1 H_2/CO, the unpromoted iron
catalyst produced almost twice the methanol as the iron nitride

catalyst. At the same conditions, the promoted iron nitride produced more total alcohol (methanol and ethanol) than the promoted iron. Nevertheless, the production of methanol by the unpromoted iron catalyst was more than the combined methanol plus ethanol produced by the K promoted iron-nitride. So, along with a lower alcohol yield, the nitride (promoted or not) was shown to produce a larger molecular weight product than iron alone.

These last two observations are in conflict to work by Anderson (1,2) with K promoted fused iron. Both Anderson and coworkers (1,2,14) plus Borghard and Bennett (15) determined that promoted iron nitride produced lower molecular weight products than an unpromoted iron catalyst. Furthermore Anderson (1,2,14) observed a significant tendency of the nitride to produce alcohols and other oxygenated products. Obviously, such discrepencies are of importance and warrant further study.

2.2 SUMMARY OF RESULTS

Unsupported ϵ-iron nitride was synthesized and the behavior of the bulk sample followed during synthesis reaction in $3H_2/CO$ at 523 K. Mössbauer paramcters of this approximate $Fe_{2.7}N$ composition were estimated as: IHS (Hyperfine Splitting) about 235 kOe and IS about 0.3 mm/s. Appearence of an additional phase, similar to that encountered in γ'-nitride $3H_2/CO$ carburization, was isolated as evidence of bulk modification. Carburization of a γ'-Fe_4N sample with $3CO/H_2$ at 523 K proceeded at a slower rate than carburization of a γ'-nitride in $3H_2/CO$. The reaction in

3CO/H$_2$ exhibited notable stability with high alkene production during four hours of reaction.

Mass Spectrometric studies revealed unique denitriding behavior of both the γ′ and the ε bulk nitrides in H$_2$. Evidence of two distinct nitrogen containing species appears; one a fast reacting surface species, and the other a slowly activating nitride species. Denitriding in helium of ε-Fe$_{2.7}$N is considerably less active, and an overall activation energy of 41.5 kcal/mol was determined. These results have significant implications to nitride stability during the Fischer-Tropsch reaction. At the onset of synthesis gas, only a small amount of NH$_3$ is observed, indicating the stability of the nitrided catalyst in CO/H$_2$ atmospheres. Additionally, if the carburized nitride is then exposed to H$_2$, the denitriding activity is surprisingly inhibited.

2.2.1 ε-Fe$_x$N Carburization

A bulk ε-iron nitride was prepared both in the Mössbauer cell and in the transient kinetics reactor. Conditions have been established for ε-Fe$_x$N production from reduced α-Fe as 673 K in 88.5%NH$_3$. We have already determined that at 673 K, 85% ammonia will produce γ′-Fe$_4$N and about 89% ammonia will produce ζ-Fe$_2$N in the Mössbauer cell (12). The present difference in synthesis conditions is attributed to slightly different precursor preparation procedures (12). Figure 1A presents the Mössbauer spectrum for the _in situ_ ε-iron nitride. Slight outer shoulders at
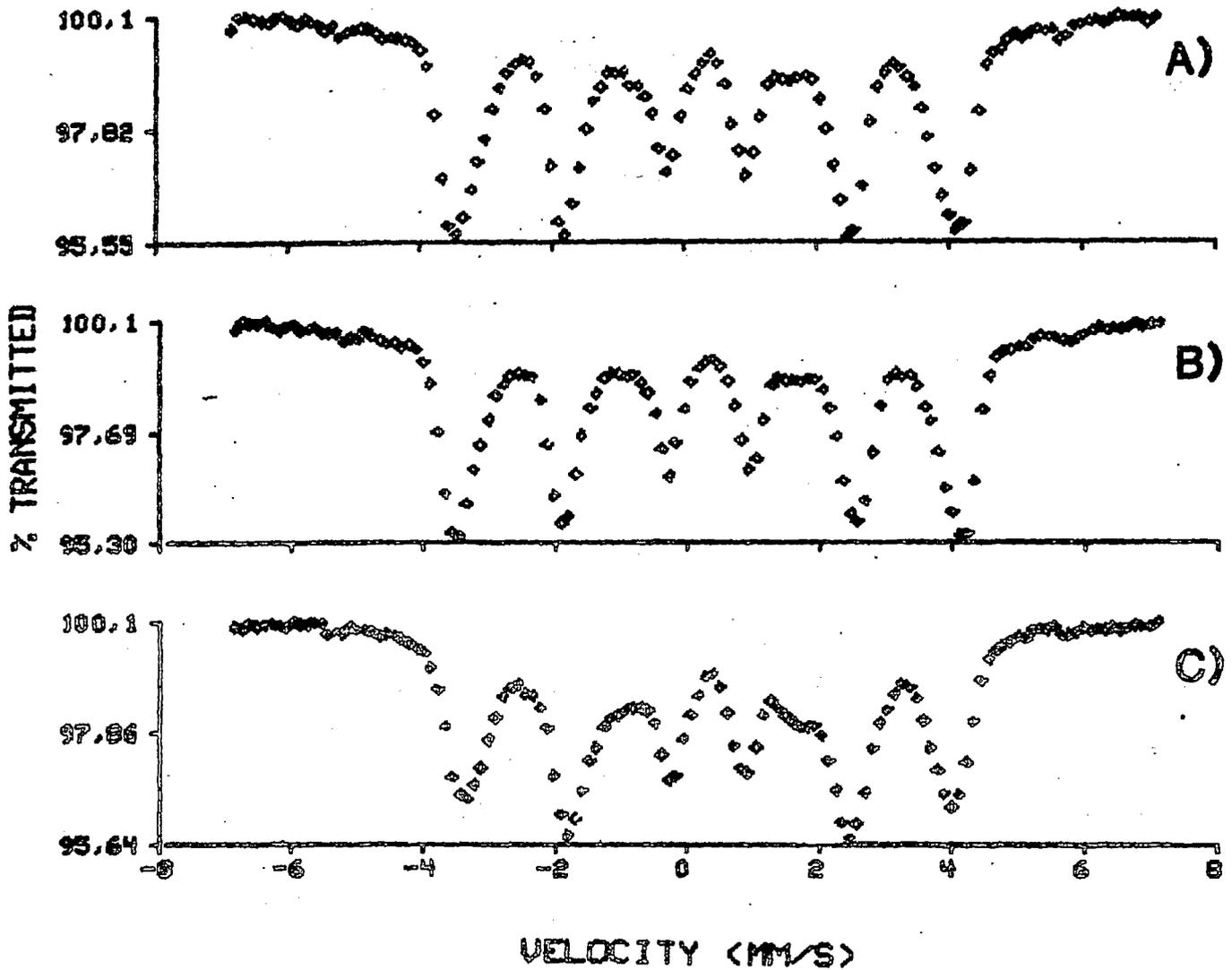
Figure 1: Mössbauer spectra (298 K) of carburization of e-Fe$_2$-N.
A) Starting e-Fe$_2$-N B) after 0.3 hr carburization in
25% CO at 523 K and C) after 2.5 hr.

approximately +5.6 and -5.3 mm/sec indicate the presence of very small quantities of zero nearest nitrogen neighbor interstices ($\gamma'-Fe_4N$). Comparison of this spectrum with one presented by Firraro et al. (16) indicates a nitrogen to iron concentration yielding approximately $\epsilon-Fe_{2.7}N$

Our ϵ-iron nitride sample was carburized in flowing $3H_2/CO$ synthesis gas at 523 K for 0.3 and 2.3 hours. The room temperature spectra are shown in Figures 1B and 1C respectively. Liquid nitrogen spectra are also available but will not be presented here. The original (Fig. 1A) six line pattern is characterized by the outer peaks having an isomer shift (IS) of about 0.3 mm/s and a hyperfine field splitting (HFS) of about 235 kOe. The spectrum after 0.3 hr of reaction changes very little from that of the fresh nitride. Rather the morphological changes occur to a greater extent during the following two hours of reaction. Figure 1C shows noticable decrease in outer peak relative intensity. This decrease is accompanied by a slight decrease in HFS and an apparent increase in the line width of these outer peaks. Hyperfine field distributions do occur with variations in the number of iron nearest neighbors (17). Preliminary spectrum analysis of Figure 1C shows the emergence of a new six line transmission pattern (HFS $\simeq$ 170 kOe, IS $\simeq$ 0.25 mm/s). This structure has already been tentatively isolated during the carburization of $\gamma'-Fe_4N$ (13). A longer reaction time would permit easier identification of this iron site. This planned work and subsequent computer fitting of the spectra should allow phase identif-

ication either as epsilon' carbide, as proposed earlier (13), or as a nitrogen containing phase.

2.2.2 Lower H_2/CO Ratios

Preliminary experiments of nitride stability and selectivity at lower H_2/CO ratios were conducted for γ'-iron nitride. Figure 2A presents the Mössbauer spectrum of a reduced iron wafer nitrided in 50% NH_3 (70 ml total flowrate) for two hours at 673 K. The sample still contains slight quantities of α-Fe as is seen by the assymetry of the four outer most lines and inner shoulder on the right most (+ velocity) peak. Otherwise, the majority of iron is in γ'-nitride fcc coordination. Figures 2B and 2C show the room temperature Mössbauer spectra of this γ'-iron nitride carburized for 17 min and for 2.5 hours respectively. 66 ml/min of $3CO/H_2$ synthesis gas mixture flowed at 523 K. The spectrum of a similar γ'-iron nitride reacted for 2.5 hours with $3H_2/CO$ (66 ml/min) at 523 K is presented in Figure 2D for comparison. The noticable difference in the γ' spectrum after 2.5 hours of reaction at higher CO concentration over the $3H_2/CO$ mixture (Figure 2C against 2D) is the maintainance of the zero nearest nitrogen neighbor sites. The intensities of the two outermost peaks (zero neighbor) and the next innermost pair are greater after the reaction in lower hydrogen partial pressure. Greater extents of carburization in $3H_2/CO$ (4-16 hours) indicate that the loss of the more noticable outer lines in the 220 kOe six line pattern accompanies the incorporation of carbon into the
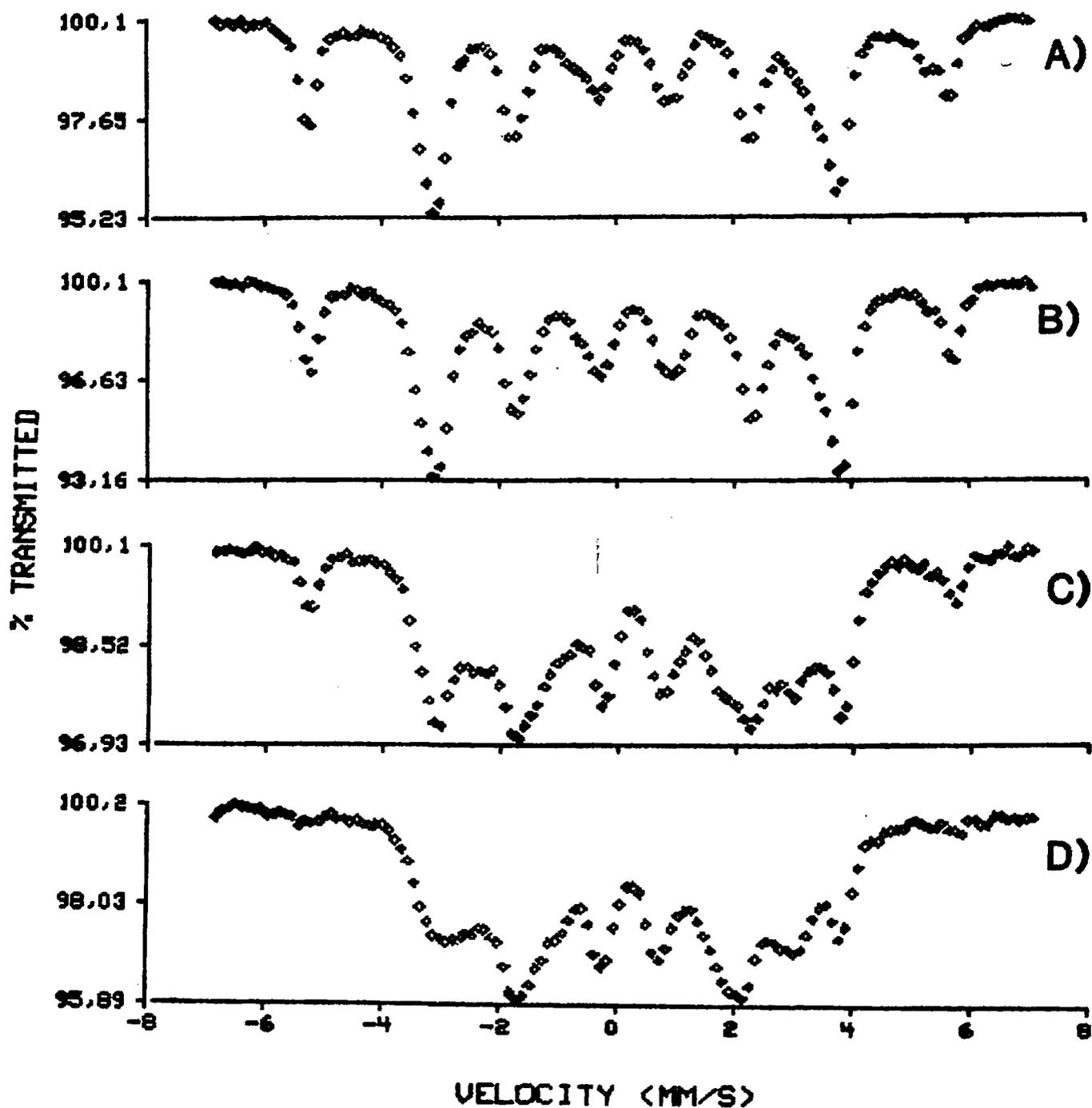
Figure 2: Mössbauer spectra (298 K) of carburization of γ'-Fe$_4$N. A) Starting γ'-Fe$_4$N B) after 0.3 hr carburization in 75% CO at 523 K and C) after 2.5 hr. D) Carburizing in 25% CO at 523 K for 2.5 hr.

nitride matrix.

On this basis, as the higher CO partial pressure is not producing an increased carburization rate, some factor must be inhibiting C incorporation. Two explainations could describe this condition. A higher overall conversion of synthesis gas to hydrocarbons (hence greater activity in equal flow comparisons) in the $3H_2$/CO experiment may produce greater active surface carbon deposition. Also, an increased partial pressure of hydrogen will provide a leaching atmosphere for substantial N removal (as NH_3), thereby providing carbon with more access to the nitride lattice. The faster rate of denitriding in H_2 than other under 'inert' conditions has been reported by Jack (10).

Kinetic analysis of the $3CO/H_2$ reaction products showed a hydrocarbon distribution high in alkenes. No noticable quantities of propane, butane nor pentane were produced during the four hour reaction. A larger ethene concentration was produced in the 75% CO flow than in the 25% CO reaction. Furthermore, the reaction was noticably more stable in $3CO/H_2$ than it had been for γ'-iron nitride exposed to 25% CO. Differences between carburization and kinetic behavior of the nitride and unpromoted iron may become more noticable at higher CO concentrations. We plan to include this avenue in our approach to elucidate the promotional affect of interstitial nitrogen upon iron in the Fischer Tropsch pathway.

2.2.3 Transient Kinetics by Mass Spectrometry

Transient denitriding behavior of both $\gamma'-Fe_4N$ and $\epsilon-Fe_xN$
has been further investigated by mass spectrometry. Figure 3
shows two separate denitriding experiments in H_2 at $250^\circ C$, one of
$\epsilon-Fe_xN$ and the other of $\gamma'-Fe_4N$. The catalysts were both
prepared from 0.1 g of Fe precursor, which was reduced and then
nitrided for 3 1/2 hours in 1) 85% NH_3/H_2 at $390^\circ C$ for $\epsilon-Fe_xN$ or
2) 75% NH_3/H_2 at $325^\circ C$ of $\gamma'-Fe_4N$. Both preparative methods were
confirmed by Mössbauer spectrometry. After being nitrided, the
catalyst was purged for several minutes with helium at $250^\circ C$ to
desorb ammonia from the system. Hydrogen, with 20% argon serving
as a time mark, was then introduced over the catalyst at a flow
rate of 50 ml/min, thereby hydrogenating the nitride as shown in
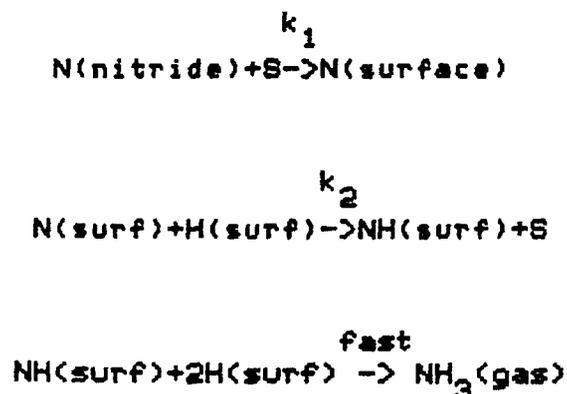Figure 3. Both catalysts had similar overall denitriding
behavior.

From the hydrogenation of Fe_4N, it is apparent that there
are two distinct nitrogen species; a first, active surface
species reacts to form the first small maximum, and then a second
slow activating species builds to a maximum after about 100
seconds. The initial small maximum represents 40% of a mono-
layer, assuming a surface area of 4.3 m^2/g reduced Fe, determined
by CO chemisorption previously (12). The large maximum is at 36%
of the total N in the catalyst. The total moles of N in the ori-
ginal catalyst is obtained by integrating the NH_3 out to ten
minutes. Accordingly, a stoichiometric formula of $Fe_{3.85}N$ is
found, which is in good agreement with a $\gamma'-Fe_4N$ catalyst.

STEP 4 H2, AR INTO HE OVER IRON NITRIDES 250C
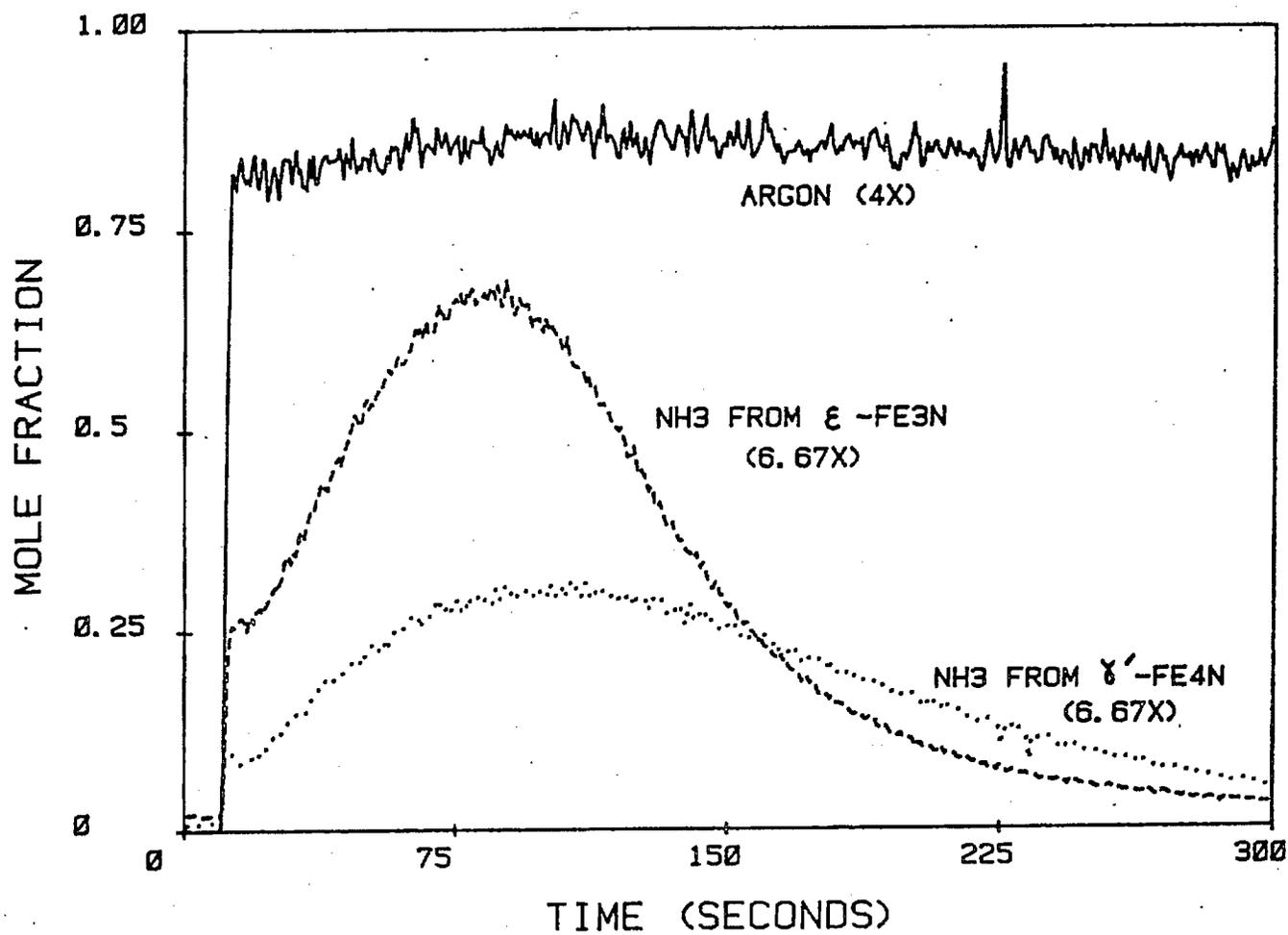
Figure 3: Denitriding of iron nitrides in H_2.

The hydrogenation of ϵ-Fe$_x$N is also shown in Figure 3. As can be seen, the activity is significantly higher for this catalyst. The initial maximum corresponds to 1.3 monolayers of material, and the large maximum is at 39% of the total N in this catalyst. In this case the stoichiometric formula is Fe$_{2.66}$N, and is therefore in the ϵ-Fe$_x$N range as expected.

If hydrogenation is diffusion limited, the evolution of ammonia is at a maximum at the onset of H$_2$, thereafter decreasing due to longer diffusion paths and decreasing area of the nitride core. Likewise, if one simple surface reaction limits the hydrogenation, then ammonia evolves at a constant rate. Figure 3 shows that neither of these models is the case. Obviously a more complex model must be proposed.

The first model considered for this process consisted of a series of irreversible surface reactions:

$$\text{N(nitride)+S} \xrightarrow{k_1} \text{N(surface)}$$

$$\text{N(surf)+H(surf)} \xrightarrow{k_2} \text{NH(surf)+S}$$

$$\text{NH(surf)+2H(surf)} \xrightarrow{fast} \text{NH}_3\text{(gas)}$$

The NH species is the precursor of the first maximum; after it is quickly hydrogenated the surface will be largely empty. A slow rise in N(surface) could presumably explain the observed

phenomenon. A first approximation for computer simulations of this model assumed that H(surface) was constant at 0.1 of a monolayer, or

$$\frac{dH(surf)}{dt} = 0$$

Results of this simulation show that this model cannot explain the extremely slow rise to a maximum, and therefore either H(surf) is not constant or the model is too simplistic. These studies are continuing.

The total duration of the denitriding processes in these experiments agrees well with similar Mossbauer experiments concerning ζ-Fe$_2$N denitriding, presented in our last report (12). While following denitriding in H$_2$ of ζ-Fe$_2$N with constant velocity Mossbauer experiments, we found that the nitride was essentially reduced after 300 seconds at 598 K, which is on a similar time scale as the denitriding of the other two nitrides shown in Figure 3. Future Mossbauer experiments will examine the structure of these nitrides during the "transition" region of the denitriding process.

When 3H$_2$/CO is added to the gas stream over virgin ϵ-Fe$_x$N at 250°C (12), ammonia is observed as a spike as in Figure 4a. If the base line NH$_3$ is subtracted, the total N observed corresponds to 1.7 monolayers, which is slightly more than that observed in pure H$_2$(1.3 monolayers). The active surface N species selectively produces NH$_3$, and further hydrogenation of the bulk

STEP CO, 3 H2, HE FROM HE OVER IRON NITRIDE
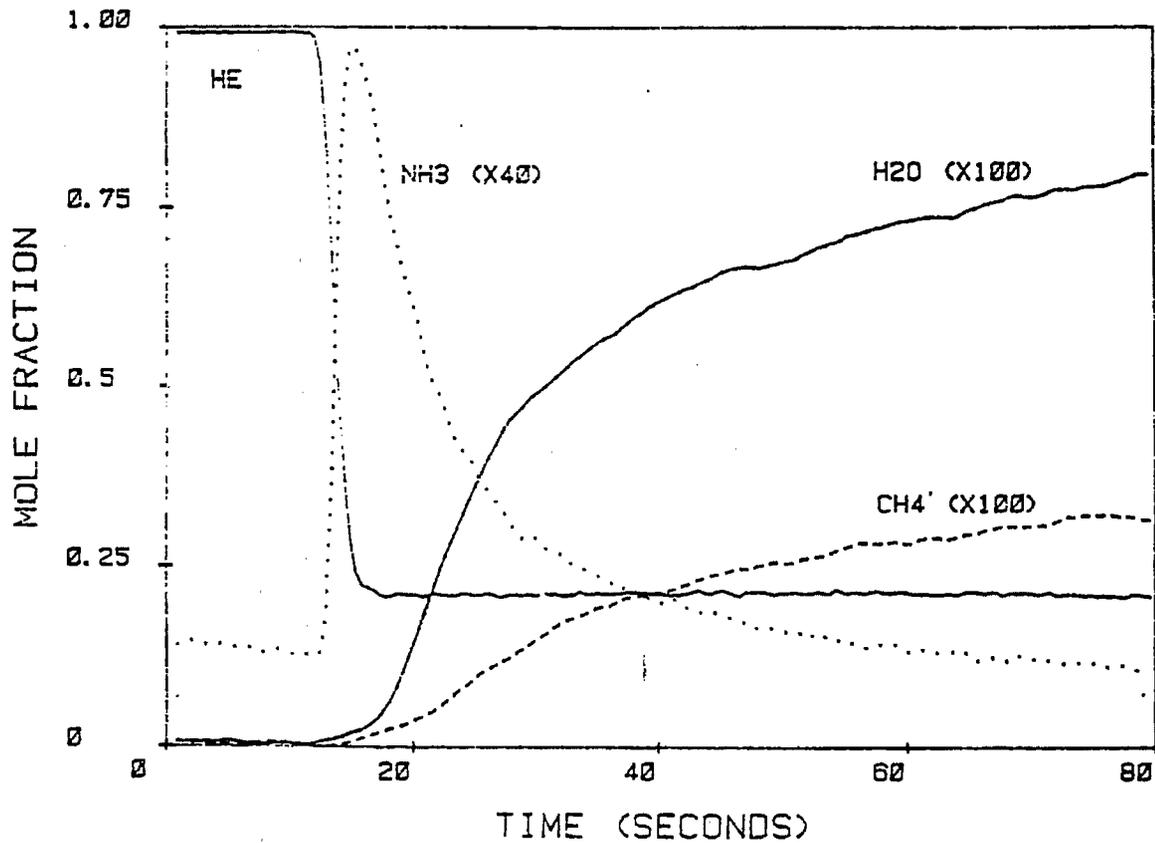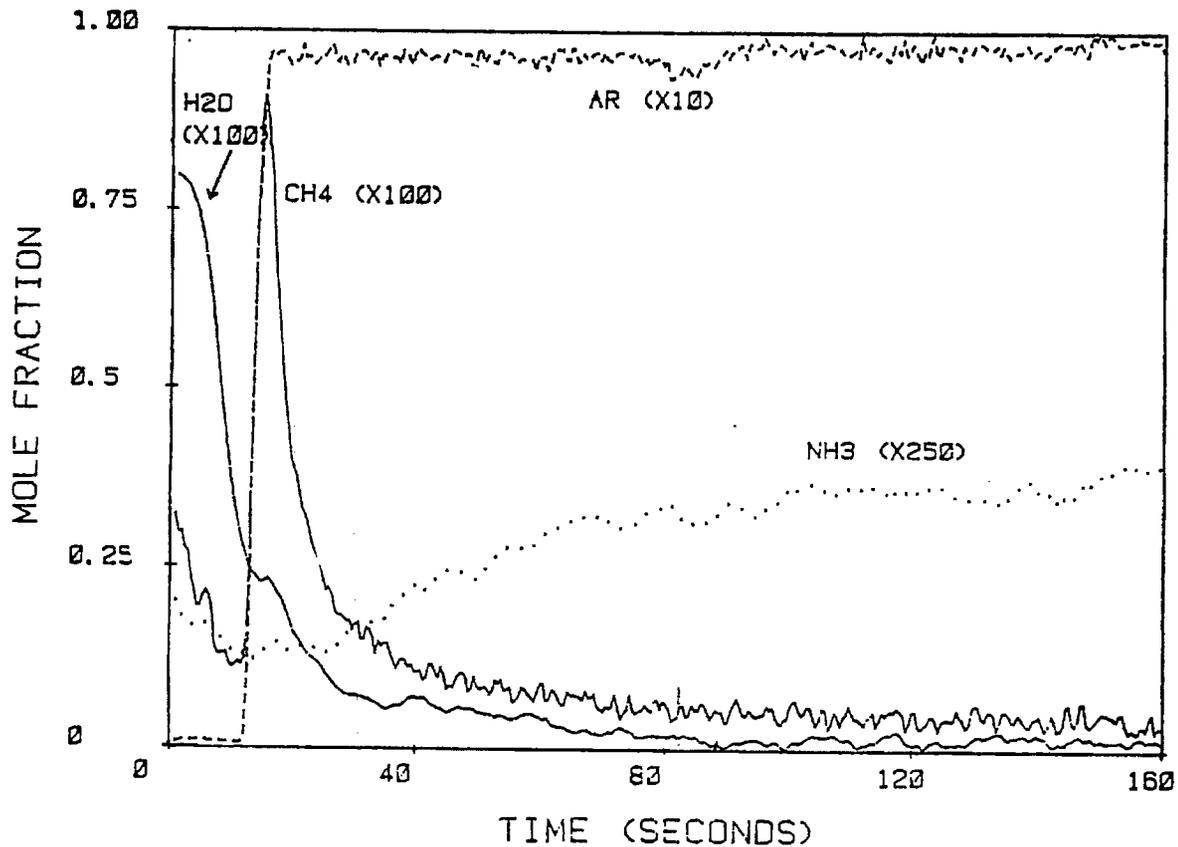

STEP 9H2, AR FROM HE AFTER FT SYNTHESIS

Figure 4: Step from He over e-Fe$_{2.2}$N to A) 3H$_2$/CO/He or B) 4H$_2$/Ar, after 5 minutes carburization.

nitride is inhibited by a surface carbon species. After five minutes of FT synthesis, the catalyst was exposed to pure H_2, and the production of NH_3 was at a constant, slow rate, as in Figure 4b. This is in contrast with the hydrogenation of virgin ϵ-$Fe_{2.7}N$ (Figure 3), in which NH_3 was produced at a much higher rate. Processes which have occured during the five minutes of synthesis clearly effect the denitriding activity.

Figure 5 shows the result of denitriding an ϵ-$Fe_{2.7}N$ catalyst in helium while ramping the temperature. The plot before 30 seconds shows the steady state nitriding conditions at $390°C$ (the NH_3 and H_2 concentrations are not shown) and the catalytic production of N_2 from NH_3 is apparent. The N_2 production corresponded to a turnover number of $5.3x10^{-2}$ sec^{-1}. Helium was then introduced over the catalyst and the temperature was ramped as shown in Figure 5. In the first portion of the graph (to the first maximum at 190 seconds), N_2 evolves according to a first order relationship and therefore an activation energy of 41.5 kcal/mol is found. This compares to Ertl et al. 's value of 26 kcal/mol for an ϵ-Fe_2N catalyst (8). The difference in stoichiometry could account for the discrepency. It is tempting to assign the second maximum to the evolution of N_2 from γ'-Fe_4N nitride formed during the denitriding process, but this needs to be studied further. Similar experiments with γ'-Fe_4N are in progress. Nevertheless, it is clear that the epsilon phase is relatively stable at temperatures below $400°C$.
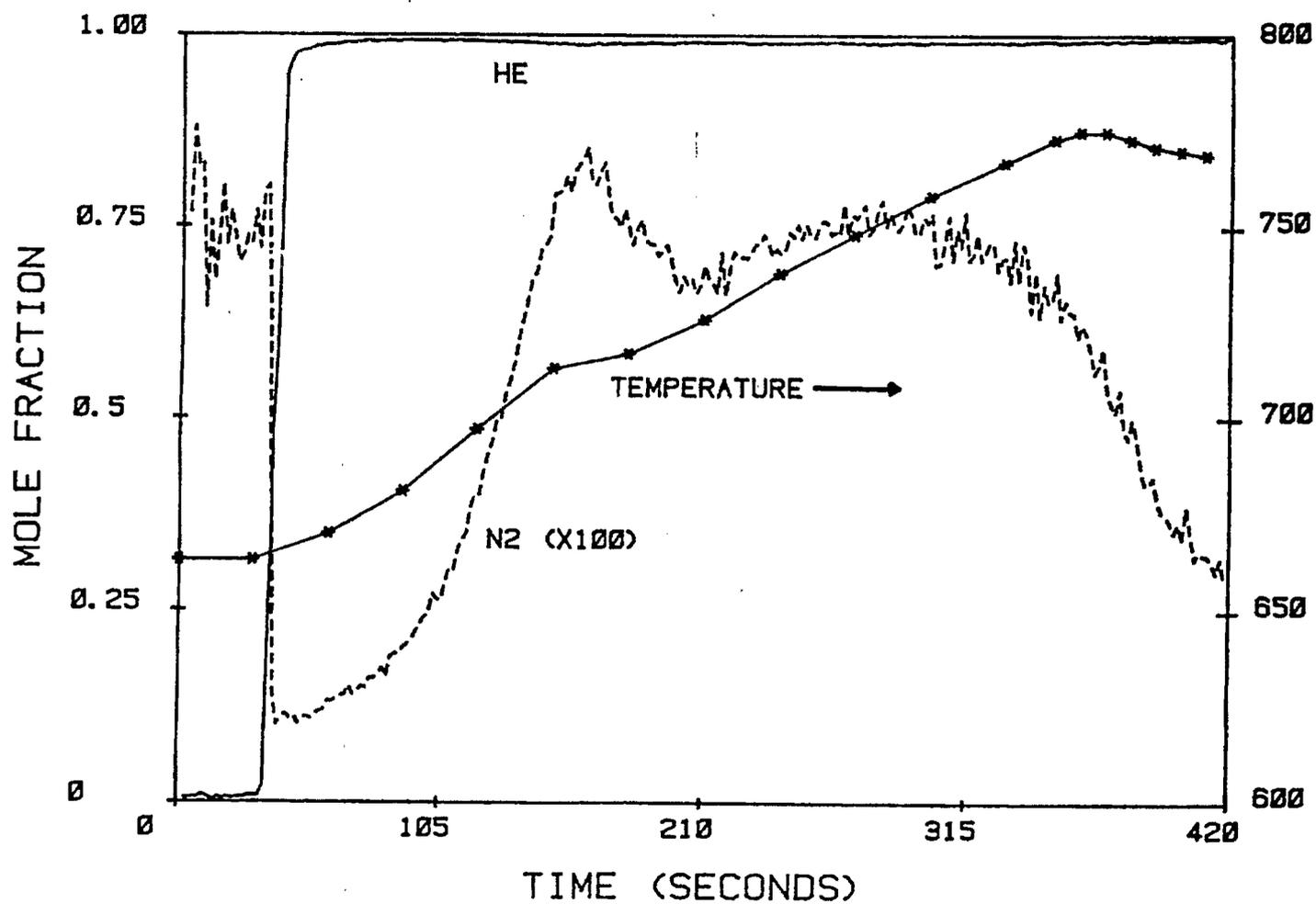
Figure 5: Denitriding of ϵ-$Fe_{2.7}N$ in He.

3. FUTURE RESEARCH

Research in the next 3 month period will emphasize higher CO (75% CO and/or 50% CO) concentrations during synthesis reactions. Stability of the nitride phases will be compared to iron reactivity under these conditions. Constant velocity Mössbauer analyses will characterize the bulk reactivity of nitride phases in less hydrogen rich atmospheres. Steady state kinetic behavior analysis coupled with computer fitting of Mössbauer spectra will aid in the identification of nitrogen movement in the catalyst.

In the transient apparatus, the kinetic denitriding behavior of ζ-Fe$_2$N will be established. The initial and steady state behavior of all the phases during Fischer- Tropsch will be further established and efforts will be made to alter this behavior by pretreatments of the nitrided catalyst.

REFERENCES

1. Anderson, R.B., Cat. Rev. - Sci. Eng. 21, 53 (1980).

2. Anderson, R.B., Adv. Catal. V 355 (1953).

3. Gainbrett, J.W. and Anvil, S.R. U.S. Patent 4272451, June 9, 1981.

4. Anvil, S.R. and Penquite, C.R., U.S. Patent 4272452, June 9, 1981.

5. Grunze, M., Bozso, F., Ertl, G. and Weiss, M., Appl. Surf. Sci. 1, 241 (1978).

6. Gay, I.D., M. Textor, R. Mason and Y. Iwasawa, Proc. Roy. Soc. (London), A365, 25 (1977).

7. Drechsler, M., Hoinkes, H., Kaarmann, H., Wilch, H., Ertl, G. and Weiss, M., Appl. Sur. Sci., 3, 217 (1979).

8.   Ertl, O., Huber, M. and Thiele, N., Z. Naturforsch, 34 A, 30 (1979).

9.   Goodeve, C. and Jack, K.H. Disc. Faraday Soc., 4, 82 (1948).

10. Jack, K.H, Proc. Roy. Soc. (London), A195, 41 (1948).

11. Engelhardt, O. and Wagner, C., Z. Phys. Chem. B18, 369 (1932).

12. U. S. Department of Energy Quarterly Technical Progress Report, DO/PC50804-4.

13. Yeh, E., Jaggi, N.K., Butt. J.B. and Swartz, L.H., (submitted).

14. Anderson, R.B., Schultz, T.F., Seligman, B., Hall, W.K. and Storch, H, J. Am. Chem. Soc., 72, 3502 (1950).

15. Borghard, W.O. and Bennett, C.O., Ind. Eng. Chem., Prod. Res. Dev. 18(1), 18 (1979).

16. Furrano, D., Rosso, M., Principi, O. and Frattini, R., I. Mat. Sc., 17, 1773 (1982).

17. DeCristofaro, N. and Kaplow, R., Met. Trans. A., 8A, 425 (1977).

U.S. DEPARTMENT OF COMMERCE
Technology Administration
National Technical Information Service
Springfield, VA 22161   (703) 605-6000